Detection of *Plasmodium falciparum*-infected red blood cells by optical stretching

Jakob M. A. Mauritz,[a,b] **Teresa Tiffert,**[b] **Rachel Seear,**[b]
Franziska Lautenschläger,[c] **Alessandro Esposito,**[a,b,*]
Virgilio L. Lew,[b] **Jochen Guck,**[c] **and**
Clemens F. Kaminski[a,d,†]

[a]University of Cambridge, Department of Chemical Engineering and Biotechnology, Pembroke Street, Cambridge, CB2 3RA, United Kingdom
[b]University of Cambridge, Department of Physiology, Development and Neuroscience, Downing Street, Cambridge, CB2 3EG, United Kingdom
[c]University of Cambridge, Department of Physics, Cavendish Laboratory, Sector of Biological and Soft Systems, J.J. Thomson Avenue, Cambridge, CB3 0HE, United Kingdom
[d]Friedrich-Alexander-Universität Erlangen-Nürnberg, School for Advanced Optical Technologies, Paul-Gordan-Str. 6, 91052 Erlangen, Germany

Abstract. We present the application of a microfluidic optical cell stretcher to measure the elasticity of malaria-infected red blood cells. The measurements confirm an increase in host cell rigidity during the maturation of the parasite *Plasmodium falciparum*. The device combines the selectivity and sensitivity of single-cell elasticity measurements with a throughput that is higher than conventional single-cell techniques. The method has potential to detect early stages of infection with excellent sensitivity and high speed. © *2010 Society of Photo-Optical Instrumentation Engineers.* [DOI: 10.1117/1.3458919]

1 Introduction

The most severe form of human malaria is caused by the parasite *Plasmodium falciparum* (*Pf*). The infection is accompanied by profound changes in the mechanical properties of the infected host red blood cells (RBCs), contributing to reduced blood flow in the microcirculation and vasoocclusion.[1] A precise assessment of the mechanical properties of infected red blood cells (IRBCs) is thus essential for an improved understanding of the disease, for the assessment of potential treatments, and for improved diagnostic purposes. At the single-cell level, micropipette aspiration, optical tweezers, and magnetic traps offer powerful tools for precise measurements of cell compliance.[2] These methods have either low

*Current address: MRC Cancer Cell Unit, Hutchison/MRC Research Centre, Hills Road, CB20XZ, Cambridge, United Kingdom
†Address all correspondence to: Clemens F. Kaminski, Department of Chemical Engineering and Biotechnology, Pembroke Street, Cambridge, CB2 3RA, United Kingdom. Tel: 44-0-1223-334777; Fax: 44-0-1223-334796; E-mail: cfk23@cam.ac.uk

throughput efficiencies or are limited in the information they yield. They are also difficult to incorporate into online diagnostic tools. Bulk methods such as ektacytometers have fast acquisition, but deliver only ensemble measurements[2,3] liable to deliver false negative results when samples contain small subpopulations of IRBCs among many uninfected cells. We report here the development and use of a novel hematological tool for the detection of IRBCs, a microfluidic optical stretcher, tested in *Pf* cultures. We show that the technique is ideally suited for the quantification of alterations in the mechanical properties of RBCs during early stages of infection. The method combines the sensitivity of traditional single-cell measurement techniques with the potential for high throughput analysis.

The optical stretcher can determine IRBC elasticity in a noncontact mode by trapping cells directly between two divergent counterpropagating laser beams.[4,5] Figure 1(a) illustrates the schematics of the setup used. The capillary and optical fibers are supported and aligned by a cross-shaped photolithographic pattern on a glass slide [Fig. 1(a)]. The trapped cell is stretched along the axis of the laser beams by simply modulating the light intensity.[4] The stretching forces are generated by the momentum transfer that occurs at the interface between the sample cell and the surrounding medium due to a change in refractive index. These surface forces pull the cell apart, analogous to a tug-of-war situation. The resulting stretching force can be 1 to 2 orders of magnitude larger than the net trapping forces, the latter arising from the asymmetric force field for cells positioned slightly off the center in the trap.[4] Spheroidal cell shapes greatly facilitate theoretical modeling, and consequently the only quantitative measurements of erythrocyte mechanical properties with the optical stretcher have been performed in the past on osmotically swollen erythrocytes.[4] To measure erythrocyte deformability without altering its original shape, the analysis of surface forces becomes more involved, but is tractable in principle using finite element method (FEM) calculations.[6] An alternative approach, taken here, is to employ a simplified phenomenological model to quantify cell compliance. Here we use the simple Kelvin-Voigt model, assuming only a global viscosity η and elasticity constant E for the whole cell. According to this model, the strain $\varepsilon(t)$ following an instantaneous constant stress σ can be described as:

$$\varepsilon(t) = a \cdot [1 - \exp(-\lambda t)], \qquad (1)$$

where $\lambda = E \cdot \eta^{-1}$ is the characteristic deformation rate and $a = \sigma \cdot E^{-1}$ is the relative amplitude of the stretch.

2 Materials and Methods

2.1 *Cultures and Preparation of Cells*

Red cells infected with *Pf* A4-BC6 clone (kindly provided by B. Elford at the Institute of Molecular Medicine, Oxford, United Kingdom), derived from clone A4, were cultured under a low-oxygen atmosphere by standard methods.[7] Parasite development and replication were assessed in cultures by microscopic inspection of Giemsa-stained thin blood smears and parasite count, as reported before.[8] IRBCs with trophozoite-stage parasites were concentrated from culture samples by
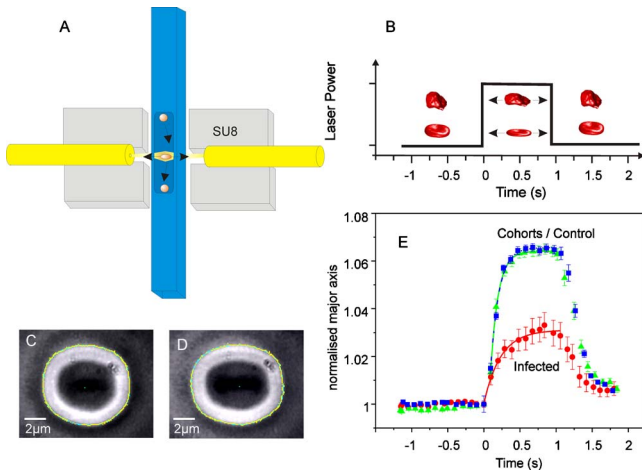
Fig. 1 (a) Schematic of the optical stretcher illustrating the photolithographical SU8 pattern used for aligning the fibers and capillary. Two lights delivering opposing fibers are automatically aligned when placed into the grooves, which are narrower than the fiber diameter. The superposition of the light creates a stable trap. Cells can be trapped and stretched, depending on the light intensity. (b) Sequence of operation during experiments. After a cell is positioned in the trap, the capillary flow is halted. The image acquisition is started and after one second the stretcher light intensity is instantaneously stepped up for approximately one second. The cells stretch and relax according to the light intensity. (c) Example of an uninfected RBC in the trap at low light power. The image analysis routine automatically locates the cell boundaries and displays corresponding cell edge pixels. (d) The same cell as in (c), elongated due to increased power in the optical stretcher. (e) Deformation behavior of uninfected RBCs compared to IRBCs. Cohorts (squares, $n=32$) and controls (triangles, $n=46$) behave similarly and exhibit small standard errors, whereas the IRBCs (circles, $n=24$) show *a* greatly reduced compliance and larger standard errors.

gelatine flotation immediately prior to experimentation. Control samples of normal, uninfected RBCs, obtained from healthy volunteers by venipuncture into a syringe with heparin, after informed written consent, were tested in parallel.

2.2 Optical Stretcher

The microfluidic optical stretcher was custom built [see Fig. 1(a)] for the IRBC experiments, modifying an integrated microfluidic design.[5] The laser beams were arranged to enter and cross the capillary 15 μm above its bottom wall. This off-center arrangement, which is lower than in previous designs, became necessary due to the rapid sedimentation of the uninfected RBCs to the capillary bottom, where they lay flat (1.5 μm height), and would otherwise not have been picked up by the optical trap. The flow capillary (number 8510, Vitrocom Limited, Mountain Lakes, New Jersey) was connected with tubing and fittings (Upchurch Scientific, Oak Harbor, Washington) to two Eppendorf reservoirs. The stretching light source was a 5-W cw linear-polarized single-mode Yb fiber laser (YLR-LP-5, IPG Photonics, Oxford, Massachusetts), emitting at a wavelength of 1070 nm. The laser light in the optical fibers (PM980-XP, Nufern Limited, East Granby, Connecticut) was split 50/50 in a polarization-maintaining Y-fiber beamsplitter (Gould Fiber Optics, Millersville, Maryland). The photolithographic pattern aligning the capillary and laser fibers was made from SU-8 2025 photoresist (MicroChem

Corporation, Newton, Massachusetts) as described in Ref. 5. The beam waist radius at the center of the trap was calculated to be $\omega \approx 14$ μm.

2.3 Stretching Procedure

The cell compliance measurements were performed as previously described.[5] When cells were trapped (with the major axis of the uninfected, biconcave-disk-shaped cells aligned parallel to the laser fibers), the flow was stopped for the time of the measurement. The laser emission was then switched on and set to a low trapping power density ($8.4 \cdot 10^5$ W/cm^2 at the trap center / 40 mW power in each fiber). The power density was instantly increased ($t_{rise} \sim 50$ μs) to $53.4 \cdot 10^5$ W/cm^2 (laser power of 2×250 mW) for one second, and then switched back to the previous lower trapping power, as sketched in Fig. 1(b). In the malaria-infected sample, cohort cells were visually distinguishable from trophozoite-containing IRBCs, as the latter contained dark hemozoin crystals and had irregular shape.[9]

2.4 Imaging and Image Analysis

The microfluidic optical stretcher was mounted on a Leica DM IRBE inverted microscope with a 63$\times$ long working distance objective (HCX-PL-FLL 63$\times$, Leica Microsystems, Wetzlar, Germany) in phase-contrast mode. The stretching sequences were recorded with a microscope camera PL-A662 (Pixelink, Ottawa, Canada) at ~ 12 frames per sec. Image analysis and edge detection were performed with custom software written in Labview Vision (National Instruments, Austin, Texas). The cell elongation was measured by performing an ellipse fit of the digitally recognized cell edge pixels, reporting the axis length parallel to the optical fibers. Figures 1(c) and 1(d) are two phase-contrast images of a stretching sequence. They show a typical sample of cell edges in trapped [Fig. 1(c)] and stretched [Fig. 1(d)] states.

3 Results/Discussion

Optical stretcher measurements of cell compliance were done in three different types of cells: 1. trophozoite-containing IRBCs, 2. uninfected RBCs of the IRBC culture (cohorts), and 3. controls. A reduced compliance was observed for IRBCs, confirming previous results obtained with optical tweezers.[10] Both cohorts and controls retained their normal biconcave disk-like shape. Figure 1(e) shows a comparison between the stretch responses of controls ($n=46$), cohorts ($n=32$), and IRBCs ($n=24$). Both uninfected samples display homogeneous behavior in the optical stretcher, with a similar compliance and a small standard error [Fig. 1(e)]. In contrast, the IRBCs are less compliant, with a relative stretch amplitude a reduced by almost half. The stretch response of IRBCs was much more variable than that of uninfected cohorts and controls, reflected in the much larger error bars.

The fitted curves in Fig. 1(e) represent the exponential strain-time relation from the Kelvin-Voigt model [Eq. (1)]. The parameters for these fits and their standard errors of the mean (SEM) are shown in Table 1.

Optical stretching of infected and uninfected red blood cells confirms results obtained with other single-cell mechanics-measurement techniques.[11] Measurements with optical tweezers had found IRBCs to stiffen significantly during

Table 1 Fitting parameters and their standard errors of the mean describing the cell deformations. The table shows the number of stretch responses n in each experiment, the two fitting parameters a and λ, the goodness of the fit (chi-square), and the average cell diameter in the trap before stretching D.

Cell type	n	a	λ (s^{-1})	χ^2	D (μm)
Infected	24	$(36 \pm 3) \cdot 10^{-3}$	2.5 ± 0.7	$8 \cdot 10^{-6}$	4.2
Controls	46	$(64 \pm 1) \cdot 10^{-3}$	9.6 ± 0.4	$2 \cdot 10^{-6}$	4.6
Cohort	32	$(66 \pm 1) \cdot 10^{-3}$	8.6 ± 0.7	$8 \cdot 10^{-6}$	4.6

parasite maturation, with shear moduli increasing up to tenfold in the late schizont stage.[11] Here we have shown that even at an early trophozoite stage, when the increase in apparent stiffness (the relative stretching amplitude a) by a factor of ~ 2 is relatively modest, IRBCs can be easily detected with the optical stretcher. Also, the values found for the elasticity-viscosity ratio (the deformation rate λ) for uninfected RBCs are in good agreement with earlier published values in the range of 5 to 10 s^{-1}.[12,13] This ratio decreased by a factor of ~ 3 for the infected cells in our experiments.

Our study shows that uninfected cohort cells from *Pf* cultures and control RBCs do not have significantly different mechanical properties *in vitro*. This is in contrast to one clinical study[3] performed with ektacytometry. Dondorp et al. attribute the reduced deformability of red blood cells (infected and uninfected) from patients with severe malaria also to alterations in the uninfected RBCs[3] (not to be confused with "uncomplicated malaria" in Ref. [3]). The ekacytometer, however, cannot distinguish between infected and uninfected RBCs. The extension to uninfected RBCs is made in that study because of the low fraction of parasitized cells present ($<20\%$), and the finding that the measured deformability did not correlate with different parasitaemia levels. It remains to be elucidated whether reduced elasticity can be observed with the optical stretcher in *ex vivo* RBC samples from patients with severe malaria.

Quantifying the absolute elasticity modulus remains an open task. It is solvable in principle and has been demonstrated for spherical shapes.[4] But the biconcave disk-like shape of uninfected RBCs, and the irregular shape of IRBCs require theoretical modeling and FEM simulations to extract absolute numbers for forces and elasticity moduli.[6] However, the simplified phenomenological model used for analysis here proved sufficient for detecting the mechanical differences in diseased cells. The characteristic deformation rate λ is independent of the actual magnitude of stress on the cell. Both parameters a and λ change significantly during infection (with the probability of the null hypothesis that the means are not different $p < 0.001$), and establish the use of this optofluidic device in applications that involve automatic cell sorting, early stage diagnostics, or screening of drugs that reduce cell stiffening.

In summary, optical stretching is a promising novel technique to measure red blood cell mechanical properties and their changes during disease. Its main advantage is that it operates entirely in a noncontact manner and can thus render results that are free from artifacts induced by adhesion to surfaces or physical contact required in other single-cell mechanical-measurement techniques. In addition, by incorporation into a suitable microfluidic environment and automation,[14] throughput rates approaching one cell per second can in principle be achieved, which compares favorably with other single-cell mechanical-measurement techniques.[5]

References

1. G. B. Nash, E. O'Brien, E. C. Gordon-Smith, and J. A. Dormandy, "Abnormalities in the mechanical properties of red blood cells caused by *Plasmodium falciparum*" *Blood* **74**(2), 855–861 (1989).
2. M. Musielak, "Red blood cell-deformability measurement: review of techniques," *Clin. Hemorheol Microcirc* **42**(1), 47–64 (2009).
3. A. M. Dondorp, B. J. Angus, M. R. Hardeman, K. T. Chotivanich, K. Silamut, R. Ruangveerayuth, P. A. Kager, N. J. White, and J. Vreeken, "Prognostic significance of reduced red blood cell deformability in severe falciparum malaria," *Am. J. Trop. Med. Hyg.* **57**(5), 507–511 (1997).
4. J. Guck, R. Ananthakrishnan, H. Mahmood, T. J. Moon, C. C. Cunningham, and J. Kas, "The optical stretcher: a novel laser tool to micromanipulate cells," *Biophys. J.* **81**(2), 767–784 (2001).
5. B. Lincoln, S. Schinkinger, K. Travis, F. Wottawah, S. Ebert, F. Sauer, and J. Guck, "Reconfigurable microfluidic integration of a dual-beam laser trap with biomedical applications," *Biomed. Microdevices* **9**(5), 703–710 (2007).
6. J. T. Yu, J. Y. Chen, Z. F. Lin, L. Xu, P. N. Wang, and M. Gu, "Surface stress on the erythrocyte under laser irradiation with finite-difference time-domain calculation," *J. Biomed. Opt.* **10**(6), 064013 (2005).
7. W. Trager and J. B. Jensen, "Human malaria parasites in continuous culture," *Science* **193**(4254), 673–675 (1976).
8. T. Tiffert, H. M. Staines, J. C. Ellory, and V. L. Lew, "Functional state of the plasma membrane Ca2+ pump in *Plasmodium falciparum*-infected human red blood cells," *J. Physiol. (London)* **525**(Pt 1), 125–134 (2000).
9. A. Esposito, J. B. Choimet, J. Skepper, J. M. Mauritz, V. L. Lew, C. Kaminski, and T. Tiffert, "Quantitative imaging of human red blood cells infected with *Plasmodium falciparum*," *Biophys. J.* (in press).
10. S. Suresh, J. Spatz, J. P. Mills, A. Micoulet, M. Dao, C. T. Lim, M. Beil, and T. Seufferlein, "Connections between single-cell biomechanics and human disease states: gastrointestinal cancer and malaria," *Acta Biomater.* **1**(1), 15–30 (2005).
11. M. Marinkovic, M. Diez-Silva, I. Pantic, J. J. Fredberg, S. Suresh, and J. P. Butler, "Febrile temperature leads to significant stiffening of *Plasmodium falciparum* parasitized erythrocytes," *Am. J. Physiol.: Cell Physiol.* **296**(1), C59–64 (2008).
12. X. Liu, Z. Y. Tang, Z. Zeng, X. Chen, W. J. Yao, Z. Y. Yan, Y. Shi, H. X. Shan, D. G. Sun, D. Q. He, and Z. Y. Wen, "The measurement of shear modulus and membrane surface viscosity of RBC membrane with ektacytometry: a new technique," *Math. Biosci.* **209**(1), 190–204 (2007).
13. R. M. Hochmuth and R. E. Waugh, "Erythrocyte membrane elasticity and viscosity," *Annu. Rev. Physiol.* **49**, 209–219 (1987).
14. A. D. Elder, S. M. Matthews, J. Swartling, K. Yunus, J. H. Frank, C. M. Brennan, A. C. Fisher, and C. F. Kaminski, "The application of frequency-domain Fluorescence Lifetime Imaging Microscopy as a quantitative analytical tool for microfluidic devices," *Opt. Express* **14**(12), 5456–5467 (2006).